AXISYMMETRIC CONVECTION WITH A MAGNETIC FIELD

D. J. Galloway
Astronomy Centre
University of Sussex
Brighton, BN1 9QH
England

Summary

The non-linear Boussinesq equations describing axisymmetric convection in a cylinder with an initially uniform magnetic field have been integrated forward in time numerically. When the field is weak a strong central fluxrope is formed at the axis. In this case the maximum field strength can be limited either kinematically or by dynamical effects, and the equipartition prediction $B^2_{max} \sim 4\pi\mu\rho u^2$ is easily exceeded. If the field is strong oscillations can occur and hysteresis is possible as the field is increased and decreased.

1. Introduction

The interaction between convection and a magnetic field determines many features observed in the solar photosphere. Sunspots and smaller scale magnetic field elements are symptoms of the ability of convection to concentrate a weak average field into strong fluxropes. Oscillatory phenomena such as running penumbral waves can occur in the presence of a strong field. To study such effects it is necessary to solve non-linear problems, and clearly to do so in three dimensions if at all possible. The recent work of Jones, Moore and Weiss (1976) on axisymmetric convection is easily extended to include the presence of a magnetic field with average strength B_o. This problem is geometrically three-dimensional but depends mathematically on only two variables, thereby rendering itself tractable to numerical computation. The normal equations of Boussinesq convection are modified to include the effect of the Lorentz force in the vorticity equation, and in addition the electromagnetic induction equation is solved to update the magnetic field as the system is integrated forward in time.

2. The Problem

To solve the equations it is convenient to set up stream functions for the velocity and magnetic fields thus:-

$$\underline{u} = \nabla \wedge (0, \frac{\psi}{r}, 0) = (-\frac{1}{r}\frac{\partial\psi}{\partial z}, 0, \frac{1}{r}\frac{\partial\psi}{\partial r}) \, ,$$

$$\underline{B} = \nabla \wedge (0, \frac{\chi}{r}, 0) = (-\frac{1}{r}\frac{\partial\chi}{\partial z}, 0, \frac{1}{r}\frac{\partial\chi}{\partial z}) \, .$$

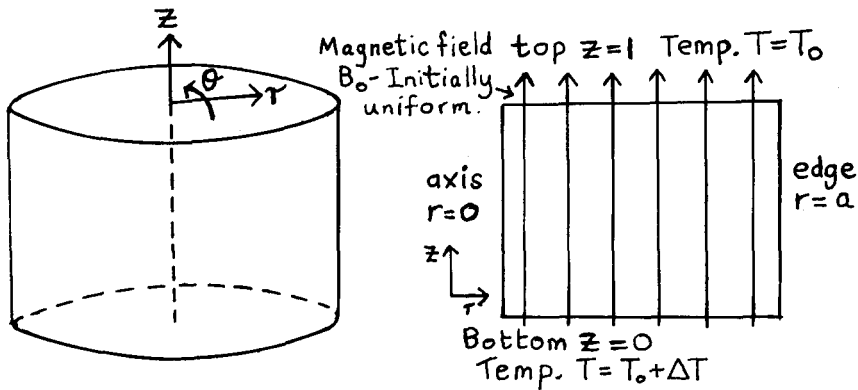We use cylindrical polar coordinates (r, θ, z). The geometry of the problem is shown in figure 1.

Fig. 1

Geometry for the axisymmetric problem, showing basic cylinder on left and axis-edge cross-section on right.

The equations $\nabla.\underline{u} = 0$ and $\nabla.\underline{B} = 0$ are automatically satisfied by the above $\underline{u}$ and $\underline{B}$ fields. Those remaining can be non-dimensionalized and put in the following form:

$$\frac{\partial\Omega}{\partial t} = -\nabla.(\Omega\underline{u}) + \frac{Q}{p_3 R}\ \nabla.(\underline{B}J)\ -\frac{1}{r}\frac{\partial T}{\partial r} + (\frac{p}{R})^{\frac{1}{2}}\ \nabla.(\frac{1}{r^2}\ \nabla(r^2\Omega))\ , \quad (2.1)$$

$$\frac{\partial T}{\partial t} = -\nabla.(T\underline{u}) + \frac{1}{(pR)^{\frac{1}{2}}}\ \nabla.(\nabla T)\ , \quad (2.2)$$

$$\frac{\partial\chi}{\partial t} = -\nabla.(\chi\underline{u}) + \frac{1}{p_3(pR)^{\frac{1}{2}}}\ r^2\nabla.(\frac{1}{r^2}\nabla\chi)\ , \quad (2.3)$$

where

$$\omega = (\nabla_{\wedge}\underline{u})_\theta = -\frac{1}{r}(\frac{\partial^2\psi}{\partial r^2} - \frac{1}{r}\frac{\partial\psi}{\partial r} + \frac{\partial^2\psi}{\partial z^2})\ = r\Omega\ , \quad (2.4)$$

$$j = (\nabla_{\wedge}\underline{B})_\theta = -\frac{1}{r}(\frac{\partial^2\chi}{\partial r^2} - \frac{1}{r}\frac{\partial\chi}{\partial r} + \frac{\partial^2\chi}{\partial z^2}) = rJ\ . \quad (2.5)$$

There are five dimensionless parameters specifying each solution to the problem; these are

$$R = \frac{g\alpha\Delta T d^3}{\kappa\nu}\ ,\ Q = \frac{B_o^2 d^2}{4\pi\mu\rho\nu\eta}\ ,\ p = \frac{\nu}{\kappa},\ p_3 = \frac{\kappa}{\eta}\ ,\ \text{and}$$

a, the ratio of cell width to cell height. The non-dimensionalization has been conducted with length scale d (layer depth), time scale $(d/g\alpha\Delta T)^{\frac{1}{2}}$, field strength scale B_o and temperature scale ΔT. The density and coefficient of volume expansion of the fluid are ρ and α; ν, κ, and η are its viscous, thermal and magnetic

diffusivities respectively, and g is the acceleration due to gravity.

The following boundary conditions are used:

$$T = T_o + \Delta T, \; B_r = 0, \; \psi = 0, \; \omega = 0 \quad (z = 0)$$

$$T = T_o , \quad\quad B_r = 0, \; \psi = 0, \; \omega = 0 \quad (z = 1)$$

$$\frac{\partial T}{\partial r} = 0, \quad \chi = \text{const.}, \; \psi = 0, \; \omega = 0 \quad (r = a)$$

$$\frac{\partial T}{\partial r} = 0, \quad \chi = 0, \quad\quad \psi = 0, \; \omega = 0 \quad (r = 0) \; .$$

The conditions on the fluid are those commonly known as stress-free. The constraint $\chi = $ const. at $r = a$ fixes the total flux in the cylinder and circumvents Cowling's theorem, so that steady solutions are possible.

The above equations and boundary conditions have been solved by finite-difference methods similar to those described in Moore, Peckover and Weiss (1973). The equations were integrated forward in time until the solutions converged to a steady state or a repeating oscillation. In many cases one solution was started from another, and in this way the effects of continuously varying one parameter could be investigated.

3. Discussion of Results

To correspond most closely with highly conducting astrophysical plasmas the program was run with values of κ/η ranging from 10 to 50. For fixed and moderately non-linear values of the Rayleigh number the following types of solution are found as Q is increased.

i)   For very weak fields the convection is unaffected and concentrates all the flux kinematically into a central rope. The structure of this rope is fixed by the balance between diffusion and advection in the induction equation. The maximum field strength B_m is higher than the input field B_o by a factor of the order of the magnetic Reynolds number, and the profile of the rope is Gaussian. Such solutions have been described by Weiss (1966) and Clark and Johnson (1967).

ii) As Q is increased a regime ensues where the imposed field remains compressed in a fluxrope but can exert a dynamical influence on the convective flow. Within the rope motion is minimal: at its edge, typically a few mesh points from the axis, there is a shear layer and the velocity reaches a value comparable with that in the absence of the field. The dynamics are dominated by a balance between the total thermal and magnetic torques; dissipation can be ohmic or viscous, and the maximum field can be successfully predicted by a power law of the form

$$\frac{B_m}{B_o} \sim \frac{R^\alpha}{Q^\beta} \left(\frac{\kappa}{\eta}\right)^\gamma \quad . \tag{3.1}$$

The numerical experiments yield average $\alpha = \beta = 0.63$ and $\gamma = 0.77$; the power-law behaviour extends over typically two orders of magnitude. The greater ability of a three-dimensional geometry to concentrate flux means it is far easier to chart this regime in the axisymmetric case than for two-dimensional rolls. It is also possible to advance physical arguments based on a boundary-layer structure (Galloway, 1976), and predict a law similar to (3.1). The exact values of α, β and γ depend on whether viscous or ohmic dissipation is dominant, and the formulae involve weakly varying logarithms, but agreement with the numerical experiments is generally very good.

An example of one of these dynamically limited solutions is shown in figure 3, which is the case $Q = 100$, $R = 20R_c$, $p = 1$, $p_3 = 10$, and $a = 4/3$. (Here $R_c = (27/4)\pi^4$). The fluxrope is almost stagnant; at its edge there is a current sheet which generates a large localized amount of negative vorticity. Within the fluxrope horizontal temperature gradients cause a very weak countercell to develop; this has an advective effect on the field and causes the fluxrope to develop a maximum some distance away from the axis. The run of the fluxrope profile as Q increases is shown in figure 2.

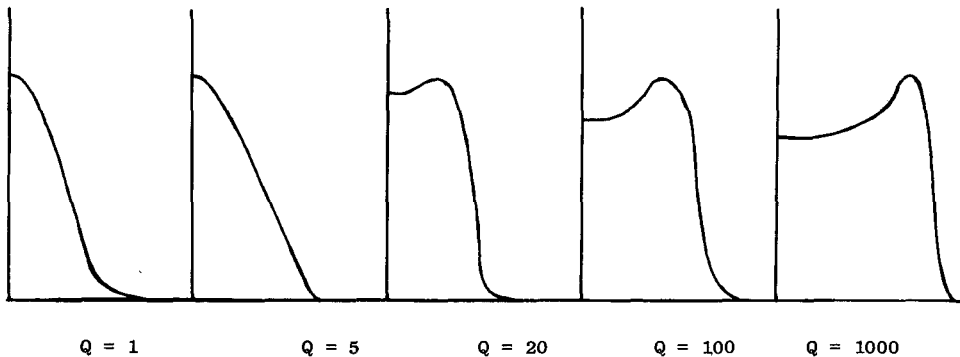| Q = 1 | Q = 5 | Q = 20 | Q = 100 | Q = 1000 |

Fig. 2.   Fluxrope profiles for $R = 20R_c$, $p = 1$, $\kappa/\eta = 10$, $a = 4/3$

iii) The central fluxrope broadens as Q is further increased and eventually it occupies about a half of the radius of the cell. At this stage the rope begins to oscillate whilst the outside circulation remains steady, and there is a corresponding variation in the heat transport. This form of solution has a natural explanation. The initially imposed field B_o is weak enough to allow steady convection, which concentrates the flux into a rope of strength B_m and radius $\frac{1}{2}a$. Flux conservation suggests $B_m \sim 4B_o$, and this means that, considered in isolation, the central rope is overstable to linear theory. The frequency of the computed solution agrees moderately well with such a linear prediction. When the senses of the two
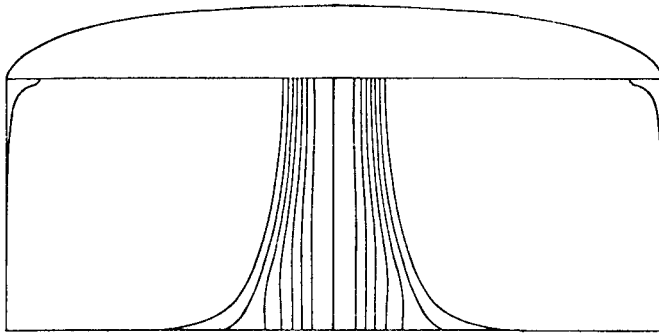
a) magnetic lines of force
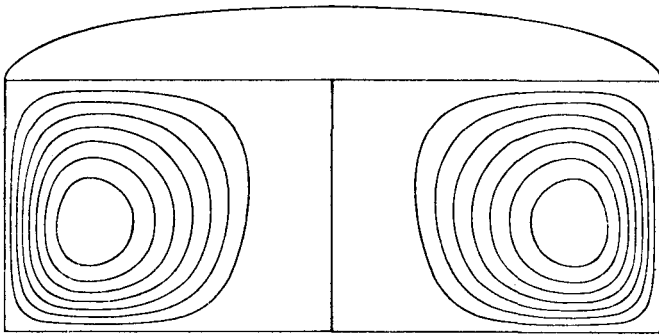
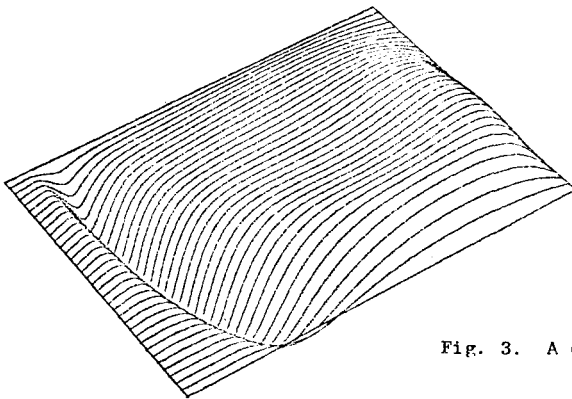b) streamlines
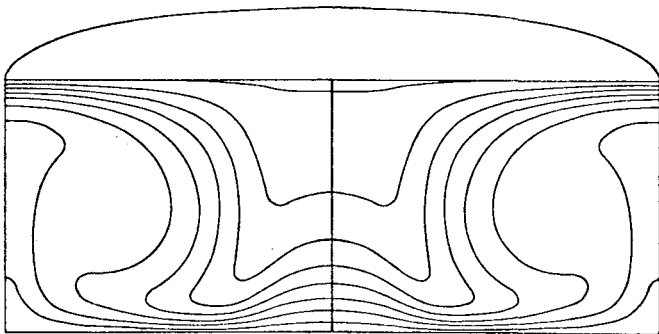
c) isotherms

d) vorticity ω (axis on left)

Fig. 3. A dynamically limited fluxrope solution.

circulations are opposite, upward moving plumes are adjacent and the heat transport
is a maximum. When the senses are the same, the cold downdraught of the countercell
is next to the hot updraught of the main flow and lateral diffusion reduces the heat
transport to a minimum.

iv) Finally Q is so strong that only finite-amplitude oscillations are possible.
These are confined mainly to the outer half of the radius, so that the solutions
are quite different to the eigenfunctions of linear theory. Periods are typically
10% - 20% faster than the linear values, presumably because the essentially quad-
ratic Lorentz term in (2.1) is badly underestimated in the linear approximation.

The nature of the solutions depends on the five dimensionless parameters defined
earlier. However there are also occasions when the system adopts a configuration
dependent on the initial conditions, so that hysteresis occurs. This effect is
encountered when the field is fairly strong. A solution with given $(Q,R,p,\kappa/\eta,a)$
can then be steady if it is part of a branch with Q increasing, and oscillatory if
part of a branch with Q decreasing - the system remembers what it was doing for
earlier values of Q. This effect can be quantified by using the Nusselt number N,
averaged in time if necessary, as a measure of the amplitude. A graph showing the
variation of N with Q as the latter is increased and decreased is shown in figure
4. For this example, Q = 10,300 marks the onset of overstability and Q = 2535 the
transition from steady to oscillatory modes according to linear theory. The slight
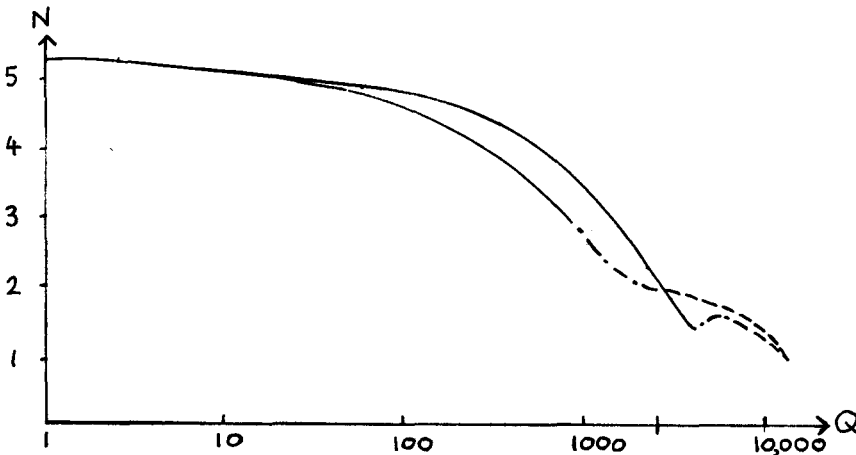<u>increase</u> in N as Q increases in the lower branch at Q = 4000 appears real.

Fig. 4. Variation of N against log Q for R = 20R_c, p = 1, κ/η = 10, a = 4/3.
------ oscillatory solution   -.-.-.- mixed steady-oscillatory solution
——— steady solution.

It is interesting to compare these hysteresis effects with the results of Huppert (1976) on double-diffusive convection, also described elsewhere in these proceedings. Broadly similar results are obtained but the magnetic results are more regular and do not show the sudden jumps in N found in the salt case. Furthermore no subcritical instabilities have yet been found in the present study.

Applications of this work to the production of intense solar magnetic fields are discussed in Galloway, Proctor and Weiss (1976). The fluxrope solutions give fields limited either by the magnetic Reynolds number or by formula (3.1); in a Boussinesq fluid the equipartition argument $B^2_{max} \sim 4\pi\mu\rho u^2$ is quite irrelevant since the pressure can adopt arbitrarily high values. The numerical results give fields up to six times greater than this prediction. We conclude that in the solar photosphere the maximum field strength is limited by the gas pressure.

Acknowledgements

References

Clark, A. and Johnson, A.C., 1967. Sol.Phys.2, 433

Galloway, D.J., Proctor, M.R.E., and Weiss, N.O. 1976. Nature, to be published

Galloway, D.J., 1976. Ph.D. Thesis, University of Cambridge

Huppert, H.E., 1976. Nature, 263, 20

Jones, C.A., Moore, D.R., and Weiss, N.O., 1976. J.Fluid Mech. 73, 353

Moore, D.R., Peckover, R.S., and Weiss, N.O., 1973. Computer Phys.Comm. 6, 198

Weiss, N.O., 1966. Proc.Roy.Soc. A, 293, 310